

¹Eui-Seok Chung, ¹B. J. Sohn*, and ²V. Ramanathan

¹Seoul National University, Seoul, Korea

²University of California, San Diego, La Jolla, California

1. INTRODUCTION

The total water vapor content in the atmosphere over the oceans can be estimated mainly from the sea surface temperature, although it is also affected by large-scale circulation (Stephens, 1990). This implies that warming induced by increases of human related greenhouse gases leads more water vapor to be evaporated from the surface into the atmosphere by the notion that the atmosphere can hold more water vapor at higher temperatures (Clausius-Clapeyron relationship). In line with this consideration present climate models show that water vapor feedback brings about an increased climate sensitivity by a factor of 2 (IPCC, 2001). This sensitivity value, however, depends on the degree of humidity of the upper troposphere under the warmer climate condition despite a small amount of water vapor in the upper layer (e.g. Lindzen, 1990).

Several studies (e.g. Soden and Fu, 1995; Udelhofen and Hartman, 1995) show a positive relationship between deep convection and upper tropospheric humidity (UTH). In contrast, some studies (e.g. Lindzen, 1990) have argued that enhanced deep convection would result in a drier upper troposphere through compensating environmental subsidence. These studies emphasize the importance of moistening processes in the upper troposphere which is considered to be one of key elements to understand water vapor feedback in the earth-atmosphere climate system.

For the better understanding of moisturizing physics in the tropical upper troposphere we examine the relationship between the convection and UTH within the deep convective cloud clusters and associated moisture changes in the surrounding area away from the deep convective cloud clusters. Satellite measurements of infrared and microwave radiation over the tropical Indian Ocean during January 1999 are used for these purposes. Together with satellite observations, the National Center for Atmospheric Research Community Climate Model (NCAR CCM3) is used as a case of reference to see if this model can produce the results obtained from satellite observation.

2. DATASETS

Meteosat 5 has been moved to its present location over the equator at 63°E to support Indian Ocean Experiment (INDOEX), hence it provides the appropriate condition for study on the relationship between deep convection related cloudiness and upper tropospheric humidity with half-hourly observation frequency. During the winter Monsoon the Intertropical Convergence Zone (ITCZ) is located in the equatorial region and corresponding subsidence branches reside over both the north and south sides of Indian Ocean. Thus, brightness temperatures from the infrared window (10.5 - 12.5 μm) and water vapor (5.7 - 7.1 μm) channel measurements during January 1999, are used for identifying clouds, determining the cloud size, and for estimating upper tropospheric humidity (UTH) over the analysis domain bounded by 25°N-35°S and 30°E-110°E. The 0.25° gridded count data processed at Laboratoire de Meteorologie Dynamique (LMD) are obtained, and then are converted into brightness temperatures using the calibration coefficients provided by European Organisation for the Exploitation of Meteorological Satellite (EUMETSAT).

Since the radiances by water vapor channel measurements are contaminated by any presence of cold clouds, the 183 GHz water vapor radiances from collocated Special Sensor for Microwave/Temperature-2 (SSM/T-2) instrument onboard Defense Meteorological Satellite Program (DMSP) F14 satellite are used for estimating the UTH within the deep convective cloud clusters.

Upper tropospheric humidity (UTH) in the 600-100 mbar layer is estimated from the water vapor radiances of both infrared and microwave channel using the relationship suggested by Soden and Bretherton (1993) and Engelen and Stephens (1998), i.e. water vapor channel brightness temperature is a linear function of the natural logarithm of UTH divided by the cosine of the viewing angle.

For the comparison of model results with satellite observations, we use NCAR CCM3 (version 3.6.6), which is a spectral general circulation model with a T42 horizontal resolution, 18 vertical levels, a 20-min time resolution, and semi-Lagrangian moisture transport scheme (Kiehl et al., 1998). Six-hourly control run outputs for perpetual January are used to determine cloud types and their respective sizes, and to estimate UTH.

* Corresponding author address: Prof. Byung-Ju Sohn, School of Earth and Environmental Sciences, Seoul National University, Seoul, 151-747, Korea; e-mail: sohn@snu.ac.kr.

3. CLOUD CLASSIFICATION

Each 0.25° Meteosat pixel is labeled as one of the following five categories, depending on infrared window brightness temperature (T_{ir}) and water vapor channel brightness temperature (T_{wv}), following Roca and Ramanathan (2000) and Roca et al. (2002). But the standard deviation of the 3×3 neighboring pixels for homogeneity check is not used because of different pixel size. (1) If $T_{ir} \leq 260K$, then pixels are regarded as convectively driven clouds including cirrus anvil clouds detrained from cumulus towers -- hereafter these clouds are referred to as deep convective clouds. (2) The pixels of $260K < T_{ir} \leq 270 K$ are regarded as mid-level clouds. (3) If $270K < T_{ir} \leq 282K$ and $T_{wv} > 246 K$, then pixels are considered as low clouds. (4) Pixels of $T_{ir} > 282 K$ and $T_{wv} > 246 K$ are called clear-sky. (5) Lastly, if $T_{ir} > 270 K$ and $T_{wv} \leq 246 K$, then pixels are labeled as semitransparent thin cirrus. Semitransparency causes clear-sky radiation complement cloud radiation, but the WV contribution peaks in the colder level (mid-to-upper troposphere) than IR case. Thus, the semitransparent thin cirrus appears colder in the WV channel than in the IR one (Roca et al., 2002). It is of importance to note that type (5) clouds are likely located in the high altitude similar to type (1) because of this reason. Fig. 1 shows an example of cloud classification for the 15th of January 1999 1500 UTC. Generally, type (2) and (3) clouds are found near type (1) clouds but type (3) clouds account for larger area coverage. Meanwhile, area coverage of type (4) clouds is underestimated compared to the result of Roca et al. (2002) because of the different classification scheme.

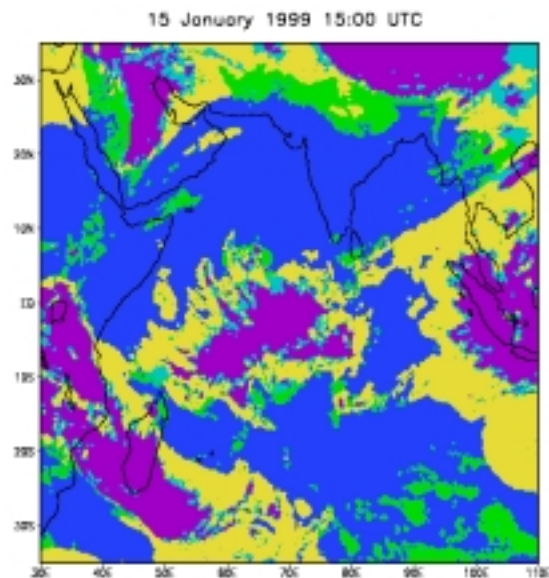


Figure 1. Example of the cloud classification result on 15 January 1999 at 1500 UTC. Deep convective cloud: violet, mid-level cloud: pale blue, semitransparent thin cirrus: yellow, low cloud: green, clear-sky: blue.

In case of CCM3, however, it is intricate to classify each grid box as one of five classes, because there are multi-level clouds and clouds often cover each grid box partially. Cloud classes of above (1) to (4) are determined by assuming the randomly overlapping clouds. Because there is no direct way to determine semitransparent thin cirrus [type (5)] from CCM3, we use different radiative forcing characteristics between optically thick and thin high clouds. Longwave cloud radiative forcing of type (1) and type (5) during January 1999, calculated using all-sky OLR and monthly mean clear-sky OLR from Meteosat 5 measurements, shows distinct difference. Longwave cloud radiative forcing of $50 W m^{-2}$ is used for dividing high clouds grids into either type (1) or type (5).

After each pixel of both Meteosat 5 and CCM3 is classified according to above criteria, a cloud clustering algorithm is applied to both Meteosat 5 and CCM3 type (1) clouds to identify cloud clusters in which individual cloud pixels share their boundaries. The total numbers of obtained cloud clusters are about 5000 for the collocated Meteosat 5 and SSM/T-2 data, and about 1600 for the CCM3 output.

4. RESULTS AND DISCUSSION

The temporal variability of the deep convective cloudiness and radiation fields is investigated. Fig. 2 shows daily time series of total deep convective cloud fraction relative to the entire domain together with domain averaged all-sky OLR from NCAR archives during January 1999. As expected, the variability of these parameters is well correlated ($R=-0.89$). Generally, OLR is inversely proportional to UTH, thus it can be expected that total deep convective cloud amount and domain averaged UTH have positive correlation. Thus, the average number of deep convective cloud clusters per each scene and UTH estimated from SSM/T-2 are presented as a function of the areal size of deep convective cloud clusters (Fig. 3). The number of deep convective cloud clusters observed in Meteosat 5 images decreases rapidly with increasing size from isolated small convective clouds to highly organized convective system like Roca and Ramanathan (2000) and Wilcox and Ramanathan (2001). But, the magnitudes are smaller by an order than that noted in Roca and Ramanathan (2000) because the analysis has been made over the collocated SSM/T-2 coverage. Meanwhile, the number of clouds counted from the CCM3 output shows a similar pattern found in satellite observations, although grid size is about ten times larger than in Meteosat 5 low-resolution dataset, indicating that both data sets show a wide spectrum of spatial scales of the deep convective cloud clusters over the tropical Indian Ocean.

The satellite observations show that the upper troposphere becomes more humid as the size of cloud cluster increases, i.e., UTH increases from about 43 % at the size of $10^3 km^2$ to 62 % at $2 \times 10^6 km^2$.

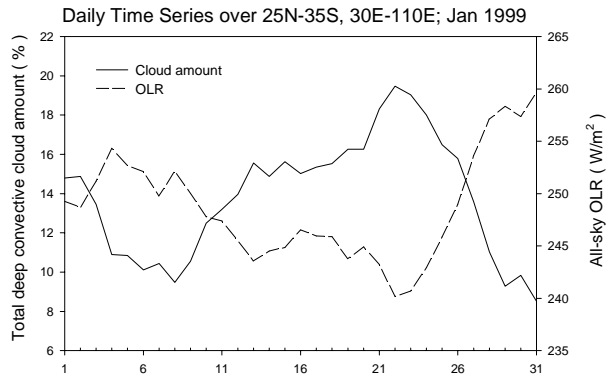


Figure 2. Daily time series of total deep convective cloud amount relative to entire domain (solid line) and domain averaged all-sky OLR (dashed line) during January 1999.

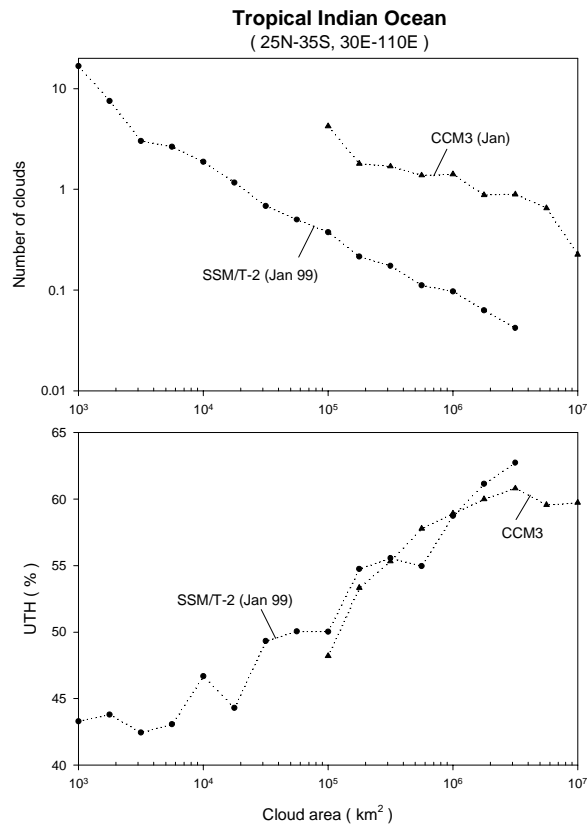


Figure 3. Distributions of (a) the average number of deep convective cloud clusters per each scene and (b) mean UTH as a function of the areal size over the Tropical Indian Ocean. Closed circles correspond to collocated SSM/T-2 and Meteosat 5 datasets during January 1999 and closed triangles represent CCM3 output during January.

The CCM3 results indicate that the model also produces moister environment as clouds become broader despite simplified treatment of moist convection processes in model. More vigorous updrafts in the deep convection core would bring more ice detrainment from the upper portion of the core and induce more outflow of evaporated water vapor associated with horizontal advection. In this way, the high UTH region spreads from the convection core. In the tropics, the locus of high UTH generally coexists with the maxima of high cloud amount for all months, because large UTH and high cloud amount are subordinate to deep convection (Soden and Fu, 1995; Chen et al., 1999), but large UTH regions may expand more than that covered with large high cloud amount. From these speculations, it can be expected that occurrence of enhanced deep convection produces broader occupation of area by cirrus anvil clouds detrained from cumulus tower, thereby causing the tropics to become more humid in a sense averaged over the entire domain.

Although increasing occupancy by deep convective cloud clusters brings more humid upper troposphere of adjacent area, whether the increase in intensity of deep convection would cause to moistening or drying of the upper troposphere over the entire tropics is the question under debate (e.g. Lindzen, 1990) because more intense deep convection leads more strong subsidence over the surrounding area through Hadley-type circulation. Fig. 4 shows the relationship between the intensity of deep convection activity and the UTH estimated from Meteosat 5 over the area classified as low cloud or clear-sky. Those regions account for about 60%, on average, of entire domain. Satellite observation indicates a decreasing trend of UTH with respect to total deep convective cloud amount, with slope of -0.16 , suggesting that stronger deep convection results in drier upper troposphere over the subsiding regions (Sohn and Schmetz, 2002). On the other hand, CCM3 represents a slight increase of UTH, with slope of 0.09 , with respect to the increase in total deep convective cloud area, although the linearity is weak. Since more intense deep convection transports water vapor from colder and drier levels downward, increasing trend of UTH seems to result from simplified treatment of moist convection processes. Meanwhile, satellite observation shows about 10% smaller UTH compared to CCM3 probably due to the dry bias of water vapor channels of Meteosat satellites (Sohn et al., 2000).

The drying rate of atmospheric column with time is reduced or even reversed when partial cloud cover present (Soden, 1998), thus it would be expected that any presence of mid-level clouds or semitransparent thin cirrus clouds represents different UTH variation pattern from that of low clouds or clear sky case. Fig. 5 shows UTH, estimated from Meteosat 5, variation with respect to total deep convective cloud area over the regions classified as mid-level clouds and semitransparent thin cirrus, respectively. Enhanced

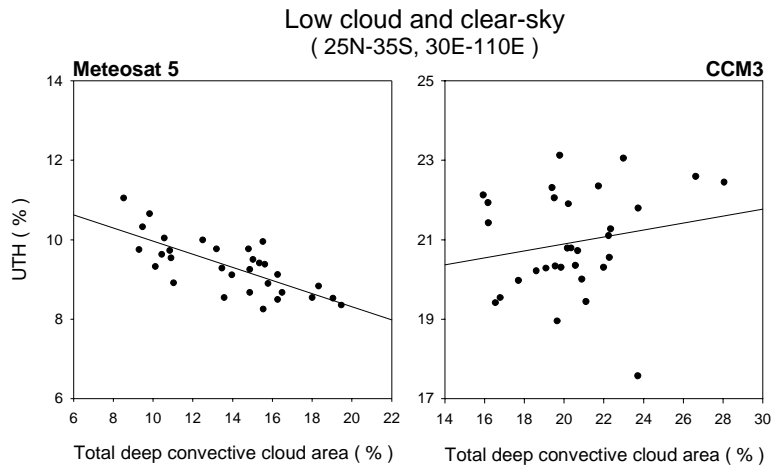


Figure 4. Variations of mean UTH of the regions of low clouds or clear-sky with respect to total deep convective cloud area over the Tropical Indian Ocean. Left panel represents collocated SSM/T-2 and Meteosat 5 datasets during January 1999 and right panel does CCM3 outputs during January. Each point corresponds to one day.

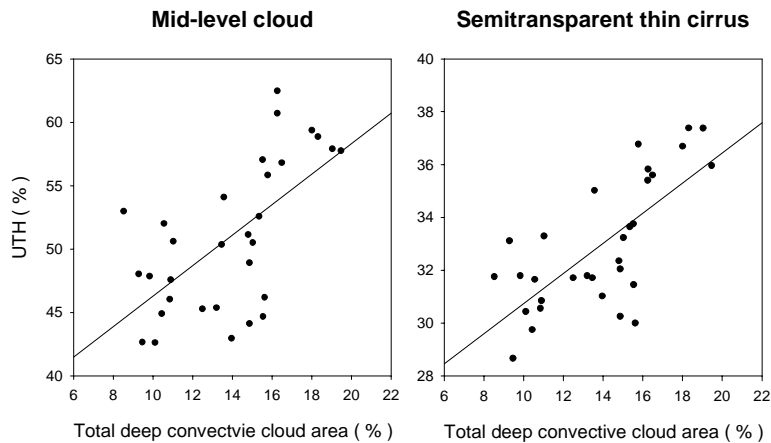


Figure 5. Variations of mean UTH estimated from Meteosat 5 with respect to total deep convective cloud area over the Tropical Indian Ocean. Left and right panel represent the region of mid-level clouds and semitransparent thin cirrus, respectively, during January 1999. Each point corresponds to one day.

deep convection leads these regions to have more humid upper troposphere with slopes of 1.20 and 0.57, respectively. Mid-level clouds consist of convection reaching lower to mid levels and the detached decaying anvil, while semitransparent thin cirrus can be associated with anvil debris (Roca et al., 2002), causing the regions of semitransparent thin cirrus to have lower UTH than the regions of mid-level clouds. However, type (2) clouds are usually found surrounding deep convective clouds with four times smaller area occupancy. Thus, the regions outside deep convective cloud clusters, what reduce drying or even moisten the upper troposphere are semitransparent thin cirrus clouds whose existence

originates from decaying detached anvil clouds or the water source left by the decay of deep convection clouds (Betts, 1990). The moistening in presence of thin cirrus could be explained through the evaporation of ice particles or through diabatic heating anomaly by cirrus clouds (Sherwood, 1999). Meanwhile, in case of CCM3, the slope for semitransparent thin cirrus case is changed considerably according to the value of longwave cloud radiative forcing used for cloud classification criterion, with larger scatter.

This study shows that semitransparent thin cirrus lessens the drying resulting from subsidence induced by deep convection and radiative cooling, but model seems to lack that process. Although model has produced similar relationship between deep convective cloud cluster size and mean UTH, the detrainment processes between deep convection and semi-transparent thin cirrus and drier upper troposphere over the regions of low clouds or clear-sky induced by enhanced deep convection have to be realized more reasonably in model, given the fact that OLR is more sensitive to the change in UTH of the subtropics than convective regions (Sohn and Schmetz, 2002).

5. REFERENCES

- Betts, A. K., 1990: Greenhouse warming and the tropical water budget. *Bull. Amer. Meteor. Soc.*, **71**, 1464-1465.
- Chen, M., R. B. Rood, and W. G. Read, 1999: Seasonal variations of upper tropospheric water vapor and high clouds observed from satellites. *J. Geophys. Res.*, **104**, 6193-6197.
- Engelen, R. J., and J. L. Stephens, 1998: Comparison between TOVS/HIRS and SSM/T-2-derived upper-tropospheric humidity. *Bull. Amer. Meteor. Soc.*, **79**, 2748-2751.
- IPCC, 2001: Climate Change 2001: *The Scientific*

- Basis. Cambridge University Press, 867 pp.
- Kiehl, J. T., J. J. Hack, B. G. Bonan, B. A. Bovill, D. L. Williamson, and P. J. Rasch, 1998: The National Center for Atmospheric Research Community Climate Model: CCM3. *J. Climate*, **11**, 1131-1149.
- Lindzen, R. S., 1990: Some coolness concerning global warming. *Bull. Amer. Meteor. Soc.*, **71**, 288-299.
- Roca, R., and V. Ramanathan, 2000: Scale Dependence of Monsoonal Convective Systems over the Indian Ocean. *J. Climate*, **13**, 1286-1298.
- Roca, R., M. Viollier, L. Picon, and M. Desbois, 2002: A multisatellite analysis of deep convection and its moist environment over the Indian Ocean during the winter monsoon. *J. Geophys. Res.*, **107**, INX2 11 1-25.
- Sherwood, S. C., 1999: On moistening of the tropical troposphere by cirrus clouds. *J. Geophys. Res.*, **104**, 11,949-11,960.
- Soden, B. J., and F. P. Bretherton, 1993: Upper tropospheric relative humidity from the GOES 6.7 μm channel: Method and climatology for July 1987. *J. Geophys. Res.*, **98**, 16,669-16,688.
- Soden, B. J. and R. Fu, 1995: A Satellite Analysis of Deep Convection, Upper-Tropospheric Humidity, and the Greenhouse Effect. *J. Climate*, **8**, 2333-2351.
- Soden, B. J., 1998: Tracking upper tropospheric water vapor radiances: A satellite perspective. *J. Geophys. Res.*, **103**, 17,069-17,081.
- Sohn, B. J., J. Schmetz, S. Tjemkes, M. Koenig, H. Lutz, A. Arriaga, and E. S. Chung, 2000: Intercalibration of the Meteosat-7 water vapor channel with SSM/T-2. *J. Geophys. Res.*, **105**, 15,673-15,680.
- Sohn, B. J., and J. Schmetz, 2002: Subtropical window counteracting water vapor area feedback: Weak 'iris' cooling effect. *J. Climate*, submitted.
- Stephens, G. L., 1990: On the Relationship between Water Vapor over the Oceans and Sea Surface Temperature. *J. Climate*, **3**, 634-645.
- Udelhofen, P. M. and D. L. Hartmann, 1995: Influence of tropical cloud systems on the relative humidity in the upper troposphere. *J. Geophys. Res.*, **100**, 7423-7440.
- Wilcox, E. M., and V. Ramanathan, 2001: Scale Dependence of the Thermodynamic Forcing of Tropical Monsoon Clouds: Results from TRMM Observations. *J. Climate*, **14**, 1511-1524.